

Behavior of Vanadium Dioxide Single Crystals Synthesized Under the Various Oxygen Partial Pressures at 1500 K

NOBORU KIMIZUKA, MOTOHIKO ISHII, ISAO KAWADA, MASANOBU SAEKI, AND MITSUOKI NAKAHIRA

National Institute for Researches in Inorganic Materials, Sakura-mura, Niihari-gun, Ibaraki-ken, 300-31, Japan

Received December 29, 1972

The effects of nonstoichiometry upon the behavior of vanadium dioxide single crystals in the vicinity of the semiconductor/metal transition temperature (T_c) were experimentally investigated. According to the electrical and thermal measurements, more stoichiometric vanadium dioxide exhibited the less electrical conductivity gap, the larger thermal and electrical hysteresis, and the lower transition temperature than the increased nonstoichiometric one near transition. Infrared absorptions and X-ray observations indicated the local and overall lattice distortion in the nonstoichiometric crystal due to the existence of V^{5+} ions. Furthermore, an intermediate phase between the low-temperature monoclinic and the high-temperature tetragonal phases was found in the nonstoichiometric VO_2 . On the other hand, no evidence for this intermediate phase was found in the stoichiometric one. Finally, some comparisons and discussions of our present data with the previously published ones were made.

Introduction

Since the 1940's, the vanadium dioxide, which shows the semiconductor/metal transition at about 70°C, has been experimentally and theoretically studied by many material scientists [for instance (1, 2)]. Also, recently, some general reviews were published by Adler and Brooks (3) and Paul (4). Although some theoretical aspects have been presented to explain the transition, the essential driving force of the transition does not appear to be well understood; some completely different models may hold depending on the materials used. One of the reasons for that may be in that the stoichiometry of the material was not well characterized in the past investigations. Prior to the present discussions, therefore, it is worthwhile making a brief summary of the previous investigations focused on the chemistry of materials used. The specimens so far investigated were prepared as follows: (a) melting V_2O_5 (mp = 670°C) either in an evacuated or in an inert gas atmosphere (for instance, He or N_2 gas) followed by single crystal growth in this V_2O_5 matrix (5), (b) mixing both V_2O_3 and V_2O_5 powders in the calculated ratio and

heating them in an evacuated silica tube at some high temperatures (6), (c) thin film (sputtered or epitaxial) (7), (d) hydrothermal method (8), (e) vapor deposition method (9), and (f) Vernouilles method (10).

The resistance discontinuity at the transition temperature, accompanied by the crystallographic change from the monoclinic to the tetragonal phase, showed the diversity between 10^1 and 10^5 (Ω cm) for various VO_2 specimens obtained using the methods described above (2, 4). The transition temperature also showed the diversity between the room temperature (11) and 70°C for these specimens.

Especially, Kennedy and Mackenzie (12) reported that their synthesized VO_2 thin film exhibited a large hysteresis and apparently even no phase transition. The phase transition of VO_2 doped with impurities of some kind was also investigated (13). Mitsuishi (14) claimed that VO_2 doped with some particular impurities showed an intermediate phase between the monoclinic and the tetragonal phases (15). Hagenmuller (16) studied the impurity effects on the transition temperature and found that

the transition temperature changed in different ways due to whether the substitution gave the V^{5+} or V^{3+} ion. The results of these investigations may supply the important information in our present studies of the effects of nonstoichiometry upon the transition.

As for the phase relation of the vanadium–oxygen system, Andersson (17) studied various oxide phases, and Roy and Kachi (18), Katsura and Hasegawa (19), and Anderson and Khan (20) investigated this system controlling the oxygen partial pressure isothermally on the basis of the Gibb's phase rule. Kimizuka, Saeki and Nakahira (21) also established the equilibrium oxygen partial pressure range of VO_2 at 1500 K and found that the range of nonstoichiometry was from $VO_{2.00}$ to $VO_{2.07}$. They have grown needle-like crystals under the controlled oxygen partial pressure (21).

The major purpose of the present work was to study the electrical and thermal behavior of VO_2 near the transition temperature using the chemically characterized specimens synthesized under the various oxygen partial pressures and to correlate this behavior with the local distortion in the nonstoichiometric VO_2 as observed through the absorption of the infrared region and the X-ray diffraction measurements. Discussion of the present data in comparison with the previously published ones is also made.

Experimental Methods

a. Preparation of the Single Crystal

As a first step, V_2O_5 powder in a Pt-crucible was reduced in CO_2 gas (99.99%) atmosphere at 1500 K for 3 days. Needle-like single crystals were grown on the wall of the crucible. Secondly, the single crystal obtained as above was put into the controlled oxygen partial pressures, $-\log P_{O_2} = 4.1, 3.5, 3.3,$ and $2.9,$ respectively, at 1500 K for 5 days to reach the equilibrium condition between the solid and the gas phases.

Every controlled atmosphere was obtained with mixing the CO_2 – H_2 gases for the lower oxygen partial pressures and CO_2 – O_2 gases for the higher oxygen partial pressures. The oxygen–vanadium ratio in the solid was determined volumetrically by adopting the Zinc–amalgam method (19, 22). The errors involved in this wet method were estimated to be within the range 0.001 through 0.002 in x of VO_{2+x} . The oxygen partial pressure in the controlled atmosphere was determined with a stabilized ZrO_2

solid-cell. In order to check the equilibrium between the gas and the solid phases, after the electrical resistance measurement of the single crystal grown under $-\log P_{O_2} = 3.3$ at 1500 K, the sample was put into the oxygen partial pressure of $-\log P_{O_2} = 4.1$ and the resistance was measured and then the atmosphere was brought back to $-\log P_{O_2} = 3.3$ and the resistance was measured again. The results obtained before and after this procedure were almost the same within the experimental error. The purity of the starting material was described elsewhere (21).

Every specimen used in this experiment was identified to be the single phase with both the X-ray powder diffraction and the Weissenberg photographic methods.

b. Electrical Resistance Measurements

The specimens used were of whisker-like single crystals and the current flow was parallel to the crystal growth direction (the a -axis of the monoclinic system). The dimensions of the specimen were approximately 7 mm in length and 0.01×0.01 mm² in cross section.

The four point probe method was used for the measurements. Contacts between the sample and the copper lead wire were bonded with silver paste and dried at room temperature for 12 hr. A sample holder (high alumina) and a chromel–alumel thermocouple were inserted into a glass tube evacuated with a mechanical pump to exclude the moisture. The sample was heated in a horizontal Khanthal wire furnace to about 100°C from room temperature. The heating and cooling rate was about 0.5°C/min. The range of the applied dc current flow to the sample was 10^{-5} to 10^{-2} mA, and in this range Ohm's law was held within the experimental error. The potential drop between the two inner probes was read with a precision vacuum-tube voltmeter.

The constancy of the dc current flow was checked using the standard resistance. The direction of the current flow was sometimes reversed to check the voltage difference. The voltage difference was noticed, but the stray thermal voltage could be estimated to be negligible. Three cycles (heating and cooling) were done to examine the hysteresis. During these processes, the samples were not broken.

c. Thermal Property Measurement

A micro-differential thermal analysis apparatus (Shimazu-Seisakusho Co.) was used. About

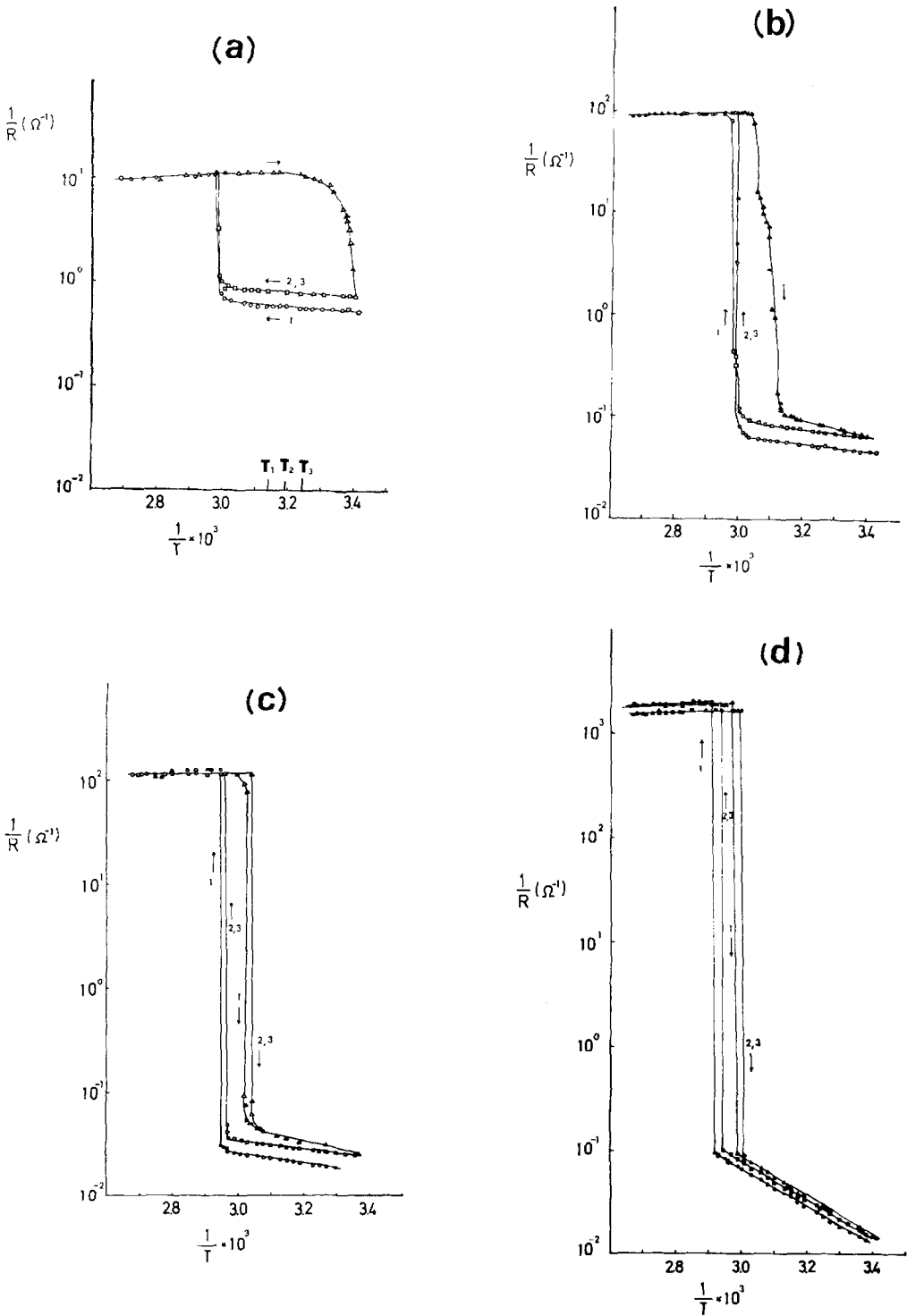


FIG. 1. The correlation between the electrical conductance and T^{-1} (K^{-1}). (a) $-\log P_{O_2} = 4.1$, $VO_{2.00}$; (b) $-\log P_{O_2} = 3.5$, $VO_{2.03}$; (c) $-\log P_{O_2} = 3.3$, $VO_{2.05}$; (d) $-\log P_{O_2} = 2.9$, $VO_{2.07}$.

10 mg of fully ground powder of VO_2 was used at each experimental run. Every operation was done in the air atmosphere. The rate of heating was $1^\circ\text{C}/\text{min}$, but the cooling rate was not controlled.

d. Infrared Absorption Measurements

Infrared absorption spectra were also measured for $\text{VO}_{2.00}$, $\text{VO}_{2.03}$, and $\text{VO}_{2.07}$ in the region from 1200 to 30 cm^{-1} . The powder samples suspended in liquid paraffin were used for the measurements of the absorption spectra. The size of the powder was about several micrometers.

Results and Discussion

a. Electrical Conductance Measurements

The observed correlations between the conductance and T^{-1} are summarized in Fig. 1 a–d. Because of the ambiguity in the potential probe distance, only the measured conductance is plotted in the figures. The check of the time dependency of the electrical conductance measurements was also made and shown in Fig. 1a. In this figure, at the temperatures indicated as T_1 ($=45^\circ\text{C}$), T_2 ($=40^\circ\text{C}$), and T_3 ($=35^\circ\text{C}$), respectively, no change in the electrical resistance was

observed during the 24 hr holding at each temperature.

Stoichiometric vanadium dioxide showed about the order of 10^1 discontinuity at T_c in the heating process, but the clear transition point was not observed in the cooling process (see Discussion on hysteresis). The conductance discontinuity at T_c became larger with increasing nonstoichiometry and the most nonstoichiometric VO_2 showed about the order of 2×10^4 discontinuity at T_c .

The conductance gap and the apparent activation energy for the conductance are summarized in Table I, and the correlations between these variables can be evaluated in Figs. 2, 3, and 4. The apparent activation energies for the conduction of the monoclinic phase are from 0.17 to 1.0 eV. Throughout these figures, it is clearly observed that the electrical conductance gap, the activation energy, and the transition temperature are raised with increased nonstoichiometry.

Comparison with the previous investigations:

Berglund and Guggenheim (2) reported the temperature dependency of the electrical conductivity using the single crystal grown from V_2O_5 matrix controlling the crystal growth rate. They

TABLE I
CONDUCTANCE GAP AT T_c AND E_a OF VARIOUS SPECIMENS

Sample	$-\log P_{\text{O}_2}^a$	Stoichiometry	T_c ($^\circ\text{C}$) ^b		T_c ($^\circ\text{C}$) ^c		$1/R_{T_c}(\Omega^{-1})^d$	E_a (eV) ^e
a	4.1	2.00	1st	63–64			1.3×10	0.17
			2nd	63–64				
			3rd	63–64				
b	3.5	2.03	1st	62–63	1st	54–55	1×10^3	0.34
			2nd	62–63	2nd	50–51		
			3rd	62–63	3rd	49–50		
c	3.3	2.05	1st	67–68	1st	57–59	5×10^3	0.22
			2nd	65–66	2nd	55–56		
			3rd	65–66	3rd	55–56		
d	2.9	2.07	1st	71–72	1st	63–64	2×10^4	1.0
			2nd	67–68	2nd	59–60		
			3rd	67–68	3rd	59–60		

^a P_{O_2} : the equilibrium oxygen partial pressure at 1500 K (atm).

^b T_c : electrical transition temperature at heating process.

^c T_c : electrical transition temperature at cooling process.

^d $1/R_{T_c}$: resistance gap at T_c .

^e E_a : the apparent activation energy for conduction of the monoclinic phase.

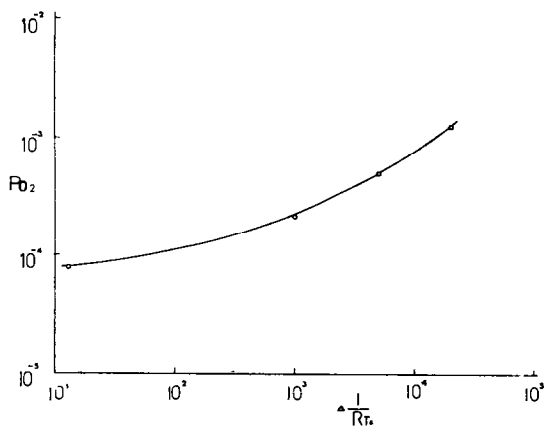


FIG. 2. The correlation between the equilibrium oxygen partial pressure (atm) and the conductance discontinuity at the transition.

showed that the sample having the larger discontinuity at T_c indicated the larger activation energy in the low-temperature phase and the less hysteresis. The activation energies from 0.65 to 0.1 eV, and the conductivity discontinuities from 8×10^4 to 2.8×10^2 in their experiments are essentially included in our present work. However, they did not describe the chemical compositions of their compounds. The fact that both the oxides, V_2O_5 and VO_2 , coexisted in the crucible at the end of the reaction means no equilibrium condition attained thermodynamically. It is likely that each sample they used may have been nonstoichiometric; namely the crys-

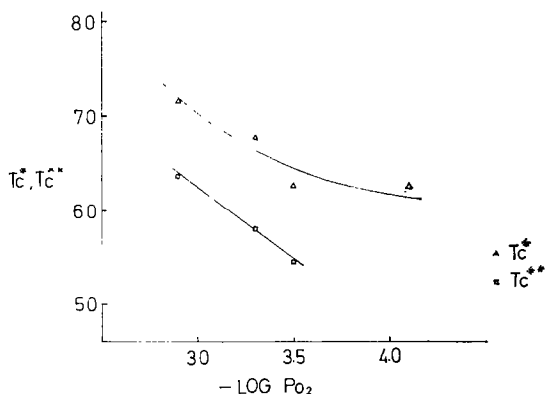


FIG. 3. The correlation between the transition temperature and $-\log P_{O_2}$. T^* ($^{\circ}C$): the transition temperature at the first heating process. T^{**} ($^{\circ}C$): the transition point at the first cooling process.

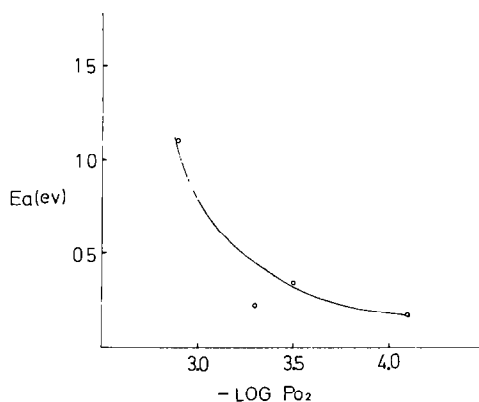


FIG. 4. The correlation between the apparent activation energy (eV) and $-\log P_{O_2}$.

tals were grown under the higher oxygen partial pressures.

MacChesney and Guggenheim (13) also claimed that the resistivity gap at T_c and its activation energy were the order of 10^4 and 0.4 eV, respectively, using the chemically characterized single crystal of $VO_{2.01 \pm 0.05}$. Their results seem to correspond to our $VO_{2.05}$ where the equilibrium oxygen partial pressure is $-\log P_{O_2} = 3.3$ at 1500 K.

Regarding the effects of the addition of impurities upon the behavior of VO_2 in the vicinity of the transition, much work has so far been done. Among them, the most systematic were of MacChesney and Guggenheim (13) and of Hagenmuller (16). In general, it appears that the smaller cations increased the resistivity gap and the larger ones decreased it. An important fact throughout these observations is that the increased addition of smaller ions which causes the displacement of these cations from the centers of the coordination octahedra produces an intermediate phase (orthorhombic or monoclinic) prior to the transition to the tetragonal phase and tends to increase the transition temperature.

Considerations on the present results:

As discussed in the following section, the infrared absorption shows the existence of V^{5+} ions in the nonstoichiometric specimens. If the nonstoichiometry means the existence of the V^{5+} ions in the octahedral sites, they are inevitably displaced from the centers of their coordination octahedra because of much smaller size, inducing the distortion of these octahedra. In terms of the electrical resistivity, it is apparent that the

increased number of V^{5+} produces an increase of positive holes, possible charge carriers, within the crystal. At the same time, however, the electrostatic balance tends to locate these V^{5+} ions adjacent to the cation vacancies which have formally negative charge. Hence, in addition to the ferroelectric displacement of the V^{5+} ions as mentioned above, this causes a large lattice polarization and will strongly trap the electrons. Judging from our present experiments, this effect overcomes the increased number of holes, resulting in the high resistivity of the nonstoichiometric specimens.

Goodenough (23) discussed the metal/semiconductor transition as due to the antiferroelectric distortion caused by the displacement of V^{4+} ions from the centers of their coordination octahedra. As in the case of the present experiments, the combination of the cation vacancy and the V^{5+} ions which causes a large local distortion will further enhance this antiferroelectric stabilization and eventually raise the transition temperature. In accordance with the effects of the addition of smaller cations, it indeed seems that these local distortions including the displacement of V^{5+} ions play an important role in the resistivity as well as the transition temperature.

Summarizing the effects of the addition of foreign cations by the previous investigators, the smaller cations raised the resistivity gap, and this can be compared with our present experiments in which increased oxidation raised the conductance gap, the activation energy of conductance, and the transition temperature. As described in the following section, the effects of impurities as described by Hagenmuller (16) in terms of the production of either V^{5+} or V^{3+} also clearly correlate with our present observations.

It is interesting to note here that the addition of only the smaller cations produces the intermediate phase as the nonstoichiometric specimens do. This suggests that the local distortion as mentioned above further increases the antiferroelectric stability. Since the chemical equilibria in terms of the oxygen partial pressure governing the incorporation of the foreign ions are complex and not known, it is not certain whether the addition of the foreign ions produces the cation vacancies. This obscures the understanding of the essential difference, if any, between the effects of nonstoichiometry and impurity addition. In fact, in the nonstoichiometric case,

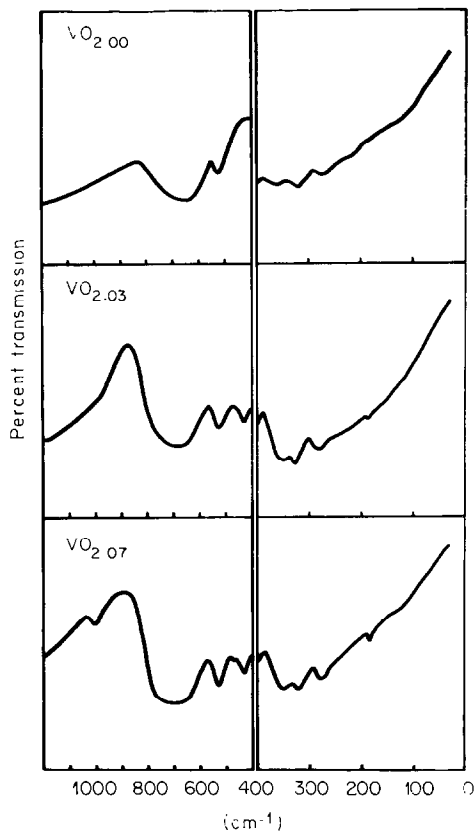


FIG. 5. Infrared absorption spectra of both the stoichiometric and nonstoichiometric vanadium dioxides.

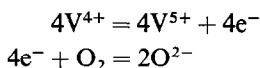
in addition to the displacement of V^{5+} ions in the octahedra the cation vacancies play an important role. However, as described above, it is evident that an enforced ferroelectric displacement of cations in both cases caused a similar effect on the transformation process.

b. Local Distortion of the Nonstoichiometric VO_2

In relation to the discussions described above, the absorption measurements of the infrared region should be mentioned here. The experimental results are summarized in Fig. 5. As shown in the figure, infrared spectra of $VO_{2.00}$ show the absorption bands in the region from 700 to 150 cm^{-1} . The low-temperature phase of VO_2 belongs to the space group $C_{2h}^5-P2_1/c$ and the Bravais unit cell contains 12 atoms; ($4VO_2$). Optically active vibrations are $9Ag + 9Bg + 8Au + 7Bu$, of which the Au and Bu modes

are active in the infrared spectra. The *Au* modes have the transition moments parallel to the *b*-axis and the *Bu* modes perpendicular to the *b*-axis. Observed bands in the region from 700 to 150 cm^{-1} are able to be assigned to these infrared active lattice vibrational modes.

Compared with the spectra of $\text{VO}_{2.00}$, an additional weak absorption band at about 1000 cm^{-1} is observed in $\text{VO}_{2.07}$. If an ionic model in VO_2 is assumed, the following equations



hold in the oxidation, and the nonstoichiometric VO_2 contains more pentavalent vanadium ions and cation vacancies in the crystal than the stoichiometric one. In comparison with the infrared absorption spectra of V_2O_5 and V_6O_{13} , which contain V^{5+} ions, the band at about 1000 cm^{-1} of the nonstoichiometric VO_2 may be of the $\text{V}^{5+}\text{-O}^{2-}$ stretching (24).

In fact, both V_2O_5 and V_6O_{13} show the bond stretching modes with the frequencies of 1000 and 900 cm^{-1} , respectively. The lengths of the $\text{V}^{5+}\text{-O}^{2-}$ bonds associated with these stretching modes are 1.59 and 1.65 Å in V_2O_5 and V_6O_{13} , respectively. The comparison between the spectra of $\text{VO}_{2.07}$ and V_2O_5 and V_6O_{13} suggests that the shortest $\text{V}^{5+}\text{-O}^{2-}$ bond length in $\text{VO}_{2.07}$ may be shorter than the shortest $\text{V}^{4+}\text{-O}^{2-}$ bond in the VO_2 lattice, resulting in the increased distortion of the coordination octahedron around the V^{5+} ion. Along with the results of the X-ray single crystal work (25), this indeed shows that the local and overall lattice distortion increase in the nonstoichiometric monoclinic VO_2 .

Hagenmuller claimed (16) that the displacement of V^{4+} by the cationic substitution of the type,



resulted in the lowering of the transition temperature. On the other hand, the transition temperature was raised by the substitution of the type,



Comparing with our present results, the transition temperature, the activation energy of the monoclinic phase, and the value of the resistance are strongly affected by the existence of V^{5+} ions in the crystal lattice.

c. Hysteresis and the Intermediate Phase of VO_2

In the first-order phase transition, hysteresis is usually observed. VO_2 is not the exception. Our results of the electrical conductance measurements show that this phenomenon is affected by the degree of nonstoichiometry (see Fig. 1 a-d). Thermally, the specimens made at the lower partial pressures at 1500 K show the very large hysteresis.

Figure 6a (1) illustrates the first heating process in which a broad exothermic peak is observed. After the temperature reached about 100°C, the specimen was cooled down rapidly to 35°C (within 30 min) and then the second heating process started with no peak up to about 100°C [Fig. 6a (2)]. It was again cooled down to room temperature and kept for 48 hr at that temperature. As shown in Fig. 6a (3), the third heating process again showed a broad peak. These observations are consistent with those of Fig. 1a, indicating a very strong hysteresis. In contrast, the most nonstoichiometric specimen showed little hysteresis and the area under the peak became broader with the increase in nonstoichiometry. Weissenberg photographs of each specimen at room temperature and those of heat-treated samples (to 100°C) have indicated the occurrence of a triclinic phase and its complicated twinning as shown in Ref. (25). The difference between the first heating process and the subsequent ones may be the effect of twinning. The two d.t.a. peaks observed for the nonstoichiometric specimen may be related to the occurrence of the intermediate phase, which appears with increasing nonstoichiometry.

The electrical behaviors corresponding to the intermediate phase were not clearly observed, but only $\text{VO}_{2.03}$ specimen showed a little different behavior from the others near the transition temperature and a small nick was observed in the vicinity of the transition temperature. Judging from these measurements, it may seem that the resistivity of the intermediate phase is more correlated to that of the monoclinic phase than the tetragonal one.

The intermediate phase has been discussed on the basis of the single crystal X-ray work (15, 25). As discussed in the previous section, the increased V^{5+} ions seem to be correlated with the appearance of this intermediate phase as shown in our present experiments as well as the Hagenmuller's report. Goodenough (23) has also discussed the two components which determine the

phase transition of this compound and concluded that the effect of the addition of impurities to the pure VO_2 compound is to separate the metal-

insulator (antiferroelectric) transition T_n and the semiconductor-semiconductor (intermediate to lower monoclinic phase) transition T_n' . The production of V^{5+} ion within the lattice may also separate the T_n and T_n' and bring about the intermediate phase. Our d.t.a. and X-ray results are consistent with his conclusions.

Summary

The results of the electrical, d.t.a., and the infrared absorption measurements, using the VO_2 specimens synthesized under the various equilibrium oxygen partial pressures at 1500 K are summarized as follows.

1. The conductance discontinuity at T_c , the activation energy of the monoclinic phase, and the transition temperature were raised with increased nonstoichiometry.

2. In comparison with the previously published data, namely the impurity effects on the behavior near T_c , the conditions of sample preparation, and the studies of ternary system containing VO_2 (for instances, $\text{VO}_2\text{-Cr}_2\text{O}_3$, $\text{VO}_2\text{-Nb}_2\text{O}_5$), a conclusion could be drawn that the nonstoichiometric effect was generally correlated to these data. A simple ionic model of VO_2 indicating the local ferroelectric distortion due to the existence of the V^{5+} ion is also related to the appearance of the intermediate phase prior to the transition.

3. Thermal and electrical hysteresis has been observed more clearly in the stoichiometric one rather than in the nonstoichiometric one.

4. Thermally, the intermediate phase was found with increased nonstoichiometry, and the results are consistent with those obtained crystallographically.

As the present experiments demonstrated, the local and overall distortions make the transition more complicated with an increase in the nonstoichiometry and the transition is not simply straightforward, depending upon the degree of nonstoichiometry. Further development of the theory should be made with this complication in mind.

References

1. F. J. MORIN, *Phys. Rev. Lett* **3**, 34 (1959).
2. C. N. BERGLUND AND H. J. GUGGENHEIM, *Phys. Rev.* **185**, 1022 (1969).
3. D. ADLER AND H. BROOKS, *Phys. Rev.* **155**, 826 (1967).
4. W. PAUL, *Mater. Res. Bull.* **5**, 691 (1970).

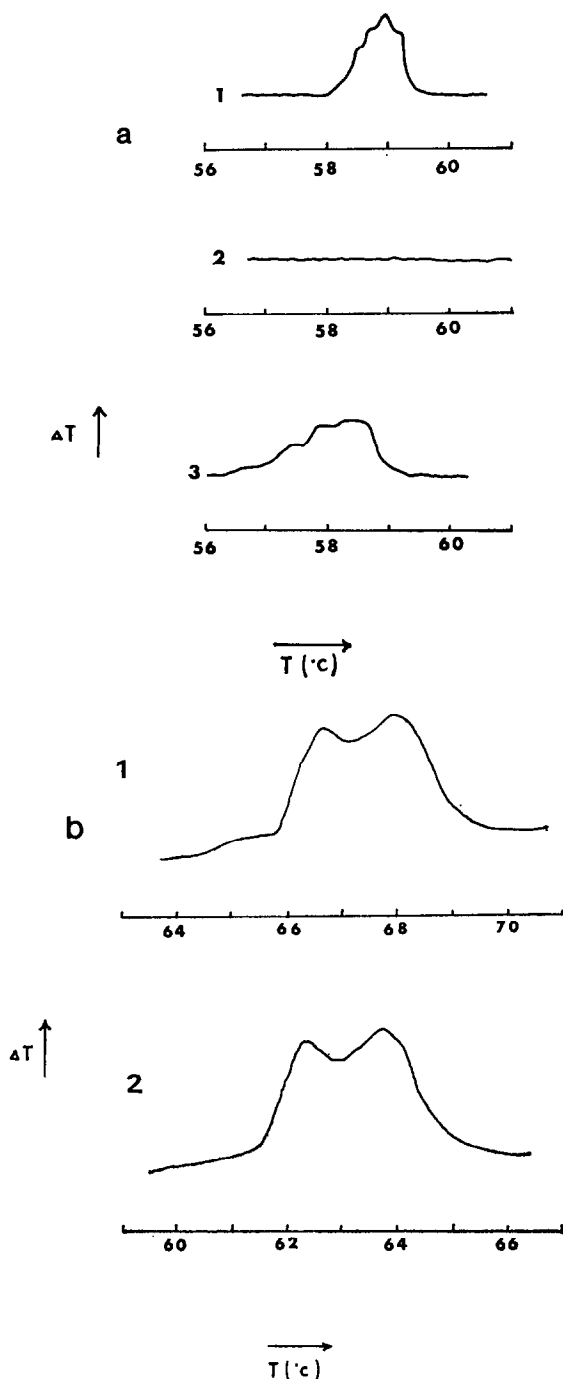


FIG. 6. The differential thermal analysis curves (a) the stoichiometric compound, $\text{VO}_{2.00}$; (b) the nonstoichiometric compound, $\text{VO}_{2.0-}$.

5. S. ARAMAKI AND R. ROY, *J. Mater. Sci.* **3**, 643 (1968).
6. T. KAWAKUBO AND T. NAKAGAWA, *J. Phys. Soc. Jap.* **19**, 517 (1964).
7. W. R. ROACH AND I. BALBERG, *Solid State Commun.*, **9**, 551 (1971).
8. R. A. LAUDIS AND J. W. NIELSEN, "Solid State Physics" (F. Seitz and D. Turnbull, **12**, p. 209. Academic Press, New York) (1961).
9. T. BANDO, *Jap. J. Appl. Phys.* **8**, 633 (1969).
10. L. E. SOBON, *Amer. Ceram. Soc. Bull.* **42**, 515 (1963).
11. W. RUEDORFF AND J. MARKLINZ, *Anorg. Allg. Chem.* **334**, 142 (1964).
12. T. N. KENNEDY AND J. D. MACKENZIE, *J. Non-Cryst. Solids* **1**, 326 (1969).
13. J. B. MACCHESNEY AND H. J. GUGGENHEIM, *J. Phys. Chem. Solids* **30**, 225 (1969).
14. T. MITSUISHI, *Jap. J. Appl. Phys.* **6**, 1060 (1967).
15. J. B. GOODENOUGH, private communication.
16. P. HAGENMULLER, *Nat. Bur. Stand. (U.S.) Spec. Publ.* **364**, 205 (1972).
17. G. ANDERSSON, *Acta Chem. Scand.* **8**, 1955 (1954).
18. R. ROY AND S. KACHI, *U.S. Army Contract Rep. No. D. A28-043AMC-01304E*, (1964).
19. T. KATSURA AND M. HASEGAWA, *Bull. Chem. Soc. Jap.* **40**, 561 (1967).
20. J. S. ANDERSON AND A. S. KHAN, *J. Less-Common Metals* **22**, 209 (1970).
21. N. KIMIZUKA, M. SAEKI AND M. NAKAHIRA: *Mater. Res. Bull.* **5**, 403 (1970).
22. I. IWASAKI, T. KATSURA, M. YOSHIDA, AND T. TARUTANI, *Jap. Anal.* **6**, 211 (1957).
23. J. B. GOODENOUGH, *J. Solid State Chem.* **3**, 490 (1971).
24. M. ISHII, I. KAWADA, AND M. NAKAHIRA, unpublished data.
25. I. KAWADA, N. KIMIZUKA, AND M. NAKAHIRA, *J. Appl. Crystallogr.* **4**, 343 (1971).